

CHAPTER 3

APPLICATION OF THE BIOSENSOR TO MEASURE ANTI-GANGLIOSIDE ANTIBODIES IN GUILLAIN-BARRÉ SYNDROME PATIENTS

3.1 Introduction

3.1.1 The Guillain-Barré syndrome

When damage occurs to the myelin sheath that protects peripheral nerves, an affliction called neuropathy results. This damage can be caused by different mechanisms like toxic substances, metabolic instabilities, other degenerative processes and also one's own immune response components like macrophages, antibodies and T-cells. The latter is known as immune-mediated neuropathies and can be further divided into chronic and acute according to the manifestation of the symptoms (Ang, 2001).

The Guillain-Barré syndrome (GBS) is the most frequent acute immune-mediated neuropathy. In the Netherlands, it is responsible for 12 deaths in a million people annually (Van Koningsveld *et al.*, 2000). It is characterised by general muscle weakness that evolves rapidly, with varying distribution and severity. It may affect respiratory muscles, causing patients to become respirator dependent. The disease reaches its most severe stage two to three weeks after onset (Hughes & Rees, 1997; Van der Meché *et al.*, 1997). Most patients recover, although residual deficiencies may be disabling. Despite intensive care unit treatment, 3-7% of all patients die (Van Koningsveld *et al.*, 2000).

A number of factors may cause the onset of GBS. Bacterial and viral infections are the most common triggers and these include *Campylobacter jejuni*, cytomegalo virus, Epstein-Barr virus, *Mycoplasma pneumoniae* and *Haemophilus influenzae*. Events that may compromise an individual's immune response, such as vaccinations and surgery, have also been suggested to trigger the onset of GBS, but this has not yet been proven with case controlled studies (Hughes, 1990; Hughes & Rees, 1997; Ang *et al.*, 2000). In both a Dutch and a British study it was observed that *C. jejuni* was the most common antecedent infection to GBS and cytomegalo virus the second most common (Table 3.1) (Winer *et al.*, 1988; Jacobs *et al.*, 1998). Distribution and frequencies of each prior infection differ between countries but in Northern China and Çuracao, *C. jejuni* is responsible for 75% of GBS cases (Ho *et al.*, 1995).

Table 3.1: The frequency of infections noted prior to the onset of GBS. (Source: Ang, 2001)

Micro-organism	Frequency
<i>Campylobacter jejuni</i>	14-66%
Cytomegalo virus	5-15%
Epstein-Barr virus	0-10%
<i>Mycoplasma pneumoniae</i>	1-11%
<i>Haemophilus influenzae</i>	1-13%

3.1.2 *Campylobacter jejuni* as antecedent infection

Campylobacter jejuni infection usually causes bloody or watery diarrhoea in humans but sometimes the infection is overlooked. Carriers of the bacterium include chickens, other meats, contaminated water, raw milk and even pets (Hudson *et al.*, 1999). The genome of *C. jejuni* is known and it has been observed that regions encoding for surface structures are highly variable. Consequently one can expect a high diversity in presentable surface antigens. In South Africa the O:41 serotype is the most common, in Japan the O:19 serotype predominates. This serotype has also been found in patients from many Western European countries (Lastovica *et al.*, 1997; Ang *et al.*, 2001b).

3.1.3 Histopathology of Guillain-Barré syndrome

Two main forms of damage occur in the nerves of patients. In the first, demyelinating GBS, macrophages infiltrating the Schwann cells of the axon can be observed as well as the presence of complement activation products (Hughes 1990; Hughes & Rees, 1997). It is thought that the sequence of events that lead to demyelination is the binding of auto-antibodies to the Schwann cells, activation of complement that forms transmembranous pores and then the removal of myelin catabolic products by the observed macrophages. In the second type, primary axonal GBS, the degeneration is observed at the node of Ranvier where the axon is bare, rather than the myelin sheath of the Schwann cells. Binding of antibodies occurs along with the lengthening of the nodal gap and complement activation again takes place (Paparounas *et al.*, 1999). Macrophages cover these nodes and invade the axonal space itself, destroying it from the root to the nerve's most distal part (Figure 3.1)

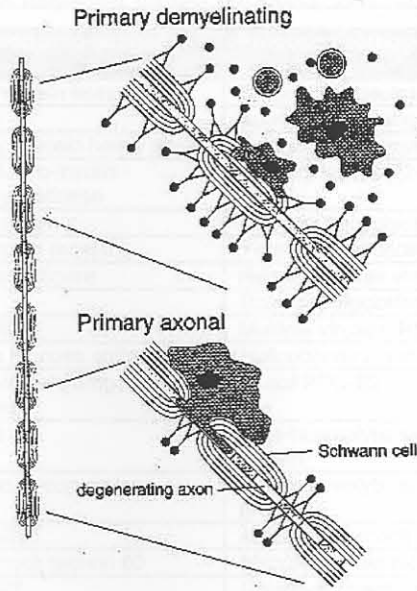


Figure 3.1: Histopathology of GBS showing macrophage invasion of the myelin sheath during demyelinating GBS and invasion of the axon during primary axonal GBS. (Source: Ang, 2001)

3.1.4 Molecular mimicry

Damian first used the term ‘molecular mimicry’ in 1964, when he referred to the antigens being similar between infectious agents and self-tissue (Damian, 1964). The mechanism can be explained as follow: antibodies are raised by the host against a certain infection. These antibodies are directed against structures on the surface of the bacterium or virus. A resemblance to surface structures of the host’s own cells would allow the antibodies to recognise the host’s own cells. This is called cross-reactivity and results in not only the infection to be destroyed but also the host’s own tissue (Albert & Inman, 1999).

The explanation of cross-reactivity is simple. We now know that almost all B- and T-cell receptors are able to recognise more than one antigen, and that the strength of interaction depends on the quality or amount of resemblance between different antigens (Van Regenmortel, 1998). Due to the amount of knowledge available on protein structure, the study of molecular mimicry has focused on the similarity between amino acid sequences (Roudier *et al.*, 1996). In a number of cases similar protein structure were found between human self-antigens and bacterial and viral antigens (Table 3.2).

Table 3.2: Diseases associated with molecular mimicry. (Source: Ang, 2001)

Immune mediated disease	Proposed auto-antigen	Proposed pathogen/molecule	Antibody/T-cell mediated
Cardiovascular disease	Alpha-myosin heavy chain	<i>Chlamydia</i> species	Both
Celiac disease	Gliadin	Adenovirus/enteric microbes	Antibodies
Chagas' disease	Cardiac myosin heavy chain	<i>Trypanosoma cruzi</i> , B13 protein	T-cells
Diabetes mellitus type 1	GAD65, pro-insulin carboxypeptidase	Coxsackievirus P2-C	T-cells
Guillain-Barré/Miller Fisher	Gangliosides	<i>C. jejuni</i> , lipopolysaccharides	Antibodies
Graves disease	Thyrotropin receptor	<i>Yersinia enterocolica</i>	Antibodies
Herpes stromal keratitis	Corneal antigens	Herpes simplex virus type 1, UL6	T-cells
Lyme diseases	LFA-1	<i>Borrelia burgdorferi</i> , OSP-A	T-cells
Multiple sclerosis	MBP/MOG	Multiple viruses: HHV-6, Epstein-Barr	Both
Peptic ulcer	Gastric mucosa antigens	<i>Helicobacter pylori</i>	T-cells
Primary biliary cirrhosis	Pyruvate dehydrogenase complex	<i>E. coli</i> PDC-E2	Antibodies
Psoriasis	Keratin	Beta-haemolytic streptococcus, M-protein	T-cells
Rheumatic heart disease	Cardiac glycoproteins	Beta-haemolytic streptococcus, M-protein	Antibodies
Rheumatoid arthritis	HLA-DRB1	40kDa heat shock protein (dnaJ)	Both
Rheumatoid arthritis	Heat shock protein 60	<i>Mycobacterium tuberculosis</i> HSP 65	Both
Spondyloarthropathies	HLA-B27	<i>Chlamydia trachomatis</i> , Gram-negative enteric pathogens	Antibodies

In GBS, the focus has been on molecular mimicry involving non-protein antigens. Not much is known about the interactions of antibodies with glycolipids or glycopeptides, but it is clear that interaction depends on the three-dimensional structure and charge of the antigen. Since it is known that a large proportion of B- and T-cells react with non-protein antigens it can be stated that cross-reaction does not exclusively depend on amino acid sequence (Van Regenmortel, 1998; Deck *et al.*, 1999). Another observation that strengthens this theory is that monoclonal antibodies can also react with completely different peptides to those they have been raised against. These peptides are called mimotopes and have the same three-dimensional structures as the target peptide (Sparbier & Walden, 1999). Monoclonal antibodies against carbohydrate antigens that react with peptides are an even more extreme case of mimicry, where the peptides have the same conformational structure as the carbohydrates (Kieber-Emmons, 1998).

3.1.5 Cholera toxin: A specific probe for ganglioside binding

Cholera toxin, an enterotoxin secreted by *Vibrio cholerae*, is responsible for the gastrointestinal manifestation of cholera (Cuatrecasas, 1973). The disease causes watery diarrhoea leading to dehydration and metabolic acidosis that, untreated, may lead to death.

The mechanism of action of CTx involves receptor-mediated binding of CTx to mucosal cells and stimulation of adenylate cyclase activity (Holmgren, 1981). The resulting

increase in cyclic adenosine monophosphate (cAMP) inhibits mainly the uptake of sodium chloride subsequently causing fluid loss (Ouchterlony & Holmgren, 1980).

Cholera toxin is a member of the family of AB₅ toxins that consist of a cell-binding domain comprised by the pentameric B subunits and a toxic domain represented by the single catalytic A subunit (Cuatrecasas, 1973). Other toxins that belong to this family include heat-labile toxin produced by *Bordetella pertussis* that causes whooping cough, Shiga and Shiga-like toxins that cause bacillary dysentery, diphtheria toxin and *Pseudomonas aeruginosa* exotoxin A (Karlsson, 1995). Figure 3.2 shows the ribbon structures of some of these AB₅ toxins and also illustrates the so-called lunar lander structure of both CTx and heat-labile toxin.

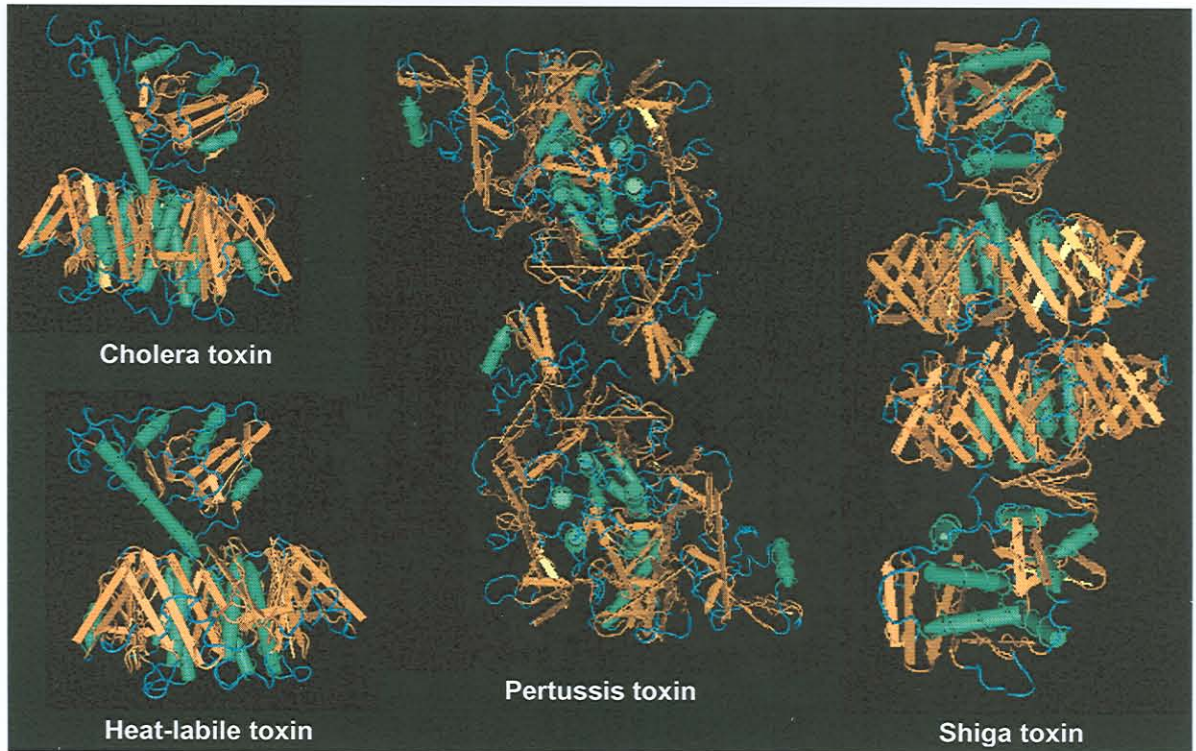


Figure 3.2: Members of the AB₅ family of toxins secreted by various bacteria. (Sources: Sixma *et al.*, 1991; Fraser *et al.*, 1994; Stein *et al.*, 1994; Zhang *et al.*, 1995)

All of these AB₅ toxins have a cell surface receptor. For CTx this is specifically G_{M1} (Cuatrecasas, 1973). Ganglioside G_{M1} binds to the B subunit of CTx in a 1:1 stoichiometry; therefore, a single CTx molecule containing five B subunits will bind to five G_{M1} molecules. Figure 3.3 illustrates the binding of the pentameric complex (cholera toxin B subunit or CTxB) to five G_{M1} molecules.



Figure 3.3: Binding of five G_{M1} molecules to the pentameric cholera toxin. (Source: Merritt *et al.*, 1994)

The G_{M1} gangliosides bind at the base of the pentamer and towards the side of the ring formed by the B subunits. The association of each ganglioside may be thought of as a two-fingered grip as a galactose- β 1,3-N-acetyl galactosamine ‘forefinger’ inserts in a pocket of the binding site and a neuraminic acid ‘thumb’ in a shallow depression (Karlsson, 1995). The ceramide tail of the G_{M1} is buried in the membrane of the host, but the arrangement of G_{M1} binding puts the G_{M1} molecules relatively far from the pore of the pentameric complex. The C-terminal tail (18 residues) of the A2 chain of the catalytic A subunit fills the central pore formed by the pentameric complex, therefore lying on top of the pore (as illustrated in Figure 4.4) and aimed away from the membrane upon binding (Karlsson, 1995). The mechanism by which the A1 fragment of the catalytic A subunit eventually crosses the host membrane to exert its cytotoxic effects remains unknown, but mechanisms available for other AB_5 toxins may provide clues to CTx’s mechanism (St Hilaire *et al.*, 1994). Nevertheless, the binding of G_{M1} to CTx and the cholera toxin is well defined, its stoichiometry known and kinetic parameters like the velocity of binding and affinity constants have been derived before (Masserini *et al.*, 1992; Kuziemko *et al.*, 1996; MacKenzie *et al.*, 1997; Athanassopoulou *et al.*, 1999). Therefore, CTx would be an ideal positive control in studies measuring the affinity of antibodies against G_{M1} .

3.1.6 Kinetics

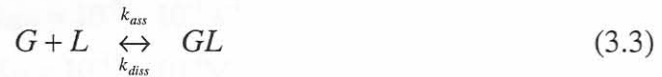
Simple binding events like one molecule of ligand (G) binding to one molecule of ligate (L), can be illustrated as follows:



The dissociation of this complex to its original state can be illustrated by:



As a whole, this interaction can be numerically described by:



where the second order association rate constant, k_{ass} , describes the rate of complex formation and the first order dissociation constant, k_{diss} , describes the rate of complex dissociation (Pathak, 1995). The actual association rate is equal to the product of the association rate constant and the concentrations of the ligand and ligate. Similarly, the dissociation rate is equal to the product of the dissociation rate constant and the ligand-ligate complex concentration. Mixing ligand and ligate in solution will result in an initial fast rate of complex formation followed by a decrease as the rate of complex formation is opposed by the rate of complex dissociation. Eventually, an equilibrium is reached where the association and dissociation rates are equal. At this point, the equilibrium can be numerically described by the equal and opposing rates, therefore:

$$k_{ass} [G][L] = k_{diss} [GL] \quad (3.4)$$

which rearranges to:

$$\frac{[G][L]}{[GL]} = \frac{k_{diss}}{k_{ass}} = K_D \quad (3.5)$$

where K_D is termed the dissociation equilibrium constant and has units M.

The constant K_D is a measure of the affinity of the ligand for the ligate and is one of the prime kinetic parameters used to describe interactions. The lower the value of K_D , the higher the affinity of a ligand for its receptor. A K_D value of 10^{-6}M would mean that at this specific ligand concentration a state of equilibrium exists between the association and dissociation rates. If this value is lower, it means that a lower concentration of ligand is necessary to reach equilibrium and implies a higher affinity. The association equilibrium constant, K_A , is the inverse of K_D but is not used as often due to more complex calculations with its inverse unit of M^{-1} (IASys, 1995b).

Typical ranges of the rate and equilibrium constants in biological samples are (IASys, 1995b):

$$k_{\text{ass}} = 10^3 - 10^7 \text{M}^{-1} \text{s}^{-1}$$

$$k_{\text{diss}} = 10^{-5} - 10^{-1} \text{s}^{-1}$$

$$K_D = 10^{-11} - 10^{-4} \text{M}$$

The interaction of the immobilised ligand with the ligate present in the injected sample is recorded using the IASys software and visualised as a standard association/dissociation curve. In order to accurately determine kinetic parameters with an interaction analysis, it is necessary to do a series of dilutions of a single test sample to generate multiple association and dissociation curves. A second program called FASTfit is then used to set the borders of the regions that should be used to calculate the kinetic parameters. Regions can be set manually or by the software, depending on the requirements of the experiment and/or user. For different concentrations the same time frame should be used for each baseline, association and dissociation region in order to calculate and compare parameters accurately (IASys, 1995b, 1996).

All the above equations assume that the ligand and ligate are present free in solutions. However, the conditions under which ligate associates with ligand are different in the IASys biosensor in a number of ways (IASys, 1995b):

- Ligand is immobilised on the sensor surface
- There is a boundary layer present between the biosensor surface and the solution
- Ligand has a relatively high concentration (μM) but low absolute amounts

- Ligand has a relatively low concentration (nM) but is in excess to ligand due to the bulk volume of the solution
- Ligand concentration remains virtually unchanged during interaction analyses
- Ligand is replenished at the biosensor surface using stirring
- Dissociation can be directly observed by removing non-bound ligand

3.1.7 Association analysis

Association curves are in fact a net result of association and dissociation events. A time frame of several minutes is usually necessary for equilibrium to be reached due to the low concentrations of ligand present. When response to added ligand increases exponentially with only one phase distinguishable, it is termed monophasic association, and biphasic association if there are two distinguishable phases (Figure 3.4). Biphasic association usually occurs at high ligand concentrations and it is possible to select whether monophasic or biphasic theoretical curves are to be used for curve fitting. The choice should depend on the quality of the theoretical curve fit. There are various ways to determine this but most often it can be done by visually comparing the two curve fits or by comparing the residual errors of both fits (IASys, 1995b).

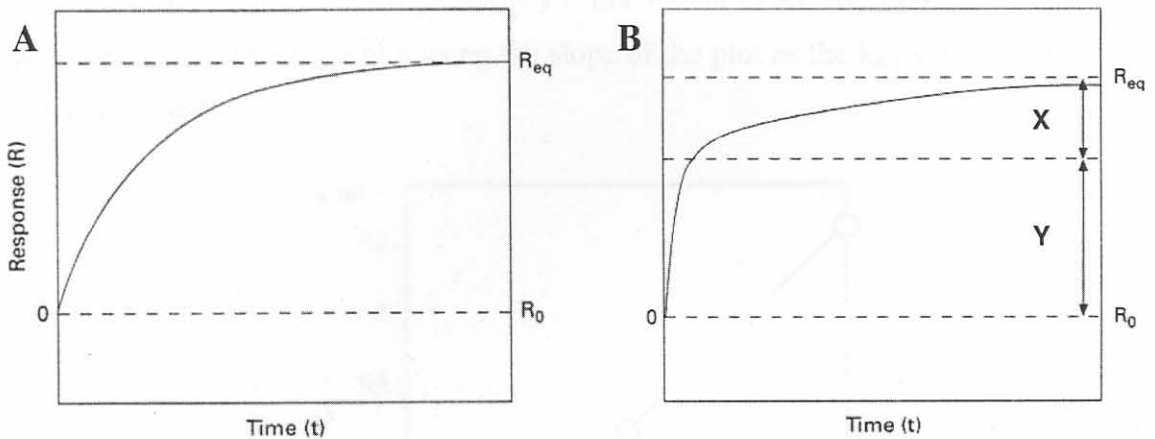


Figure 3.4: Theoretical association curves (A) Monophasic. (B) Biphasic. R_0 is the initial response, R_{eq} the equilibrium response and X and Y in graph B denotes the extents of the two phases. (Source: IASys, 1995b)

A certain amount of complex ($[GL]_t$) is formed within time t , and is described by the equation:

$$[GL]_t = [GL]_{eq} (1 - e^{-k_{on}t}) \quad (3.6)$$

where $[GL]_{eq}$ is the complex concentration at equilibrium and k_{on} is the pseudo first-order rate where:

$$k_{on} = k_{ass} [L] + k_{diss} \quad (3.7)$$

The response of the biosensor (measured in arc seconds) is related to the mass of bound ligate and is given by the equation:

$$R_t = (R_{eq} - R_0)(1 - e^{-k_{on}t}) + R_0 \quad (3.8)$$

where R_t is the response at time t , R_0 is the initial response and R_{eq} the response at equilibrium (maximum). The responses in Equation 3.8 are determined experimentally and leave the k_{on} value to be derived for a single concentration. Multiple associations carried out at different concentrations, allow the generation of a plot of k_{on} versus ligate concentration (Figure 3.5). Since k_{on} is dependent on ligate concentration and a linear relationship (Equation 3.7 is in the form $y = mx + c$) is expected, the k_{ass} and k_{diss} values can be derived from such a plot using the slope of the plot as the k_{ass} value and the y-axis intercept as the k_{diss} value.

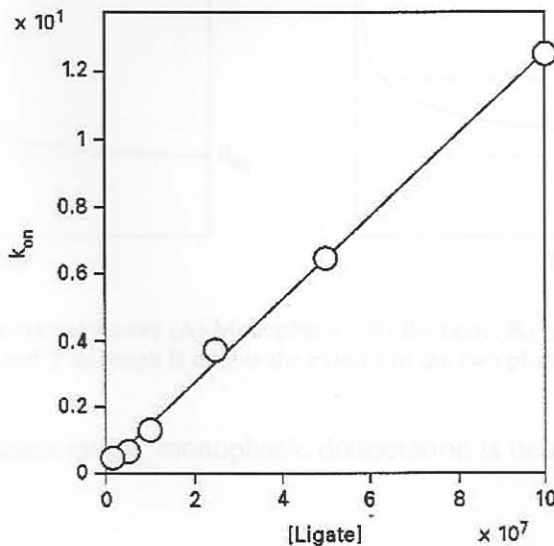


Figure 3.5: Sample plot of k_{on} versus ligate concentration. (Source: IAsys, 1995b)

In biphasic association, the total association is the sum of two individual association processes, each with its own association rate constant:

$$R_t = X(1 - e^{-k_{on(1)t}}) + Y(1 - e^{-k_{on(2)t}}) + R_0 \quad (3.9)$$

where X and Y are the extents; and $k_{on(1)}$ and $k_{on(2)}$ the apparent on-rates of the two individual and separate phases (see Figure 3.4). The slower phase, described by $k_{on(2)}$, contains no easily interpretable data; therefore $k_{on(1)}$ is used to determine k_{ass} . This faster rate constant describes binding events best when dealing with biphasic association.

The K_D value can now be calculated using the derived k_{ass} and k_{diss} constants. However, k_{diss} derived from such a plot (k_{on} vs. [ligate]), is often very close to zero and the error around the value considerable. An improvement of the k_{diss} value can be found by analysing the dissociation data.

3.1.8 Dissociation analysis

Dissociation events can also exhibit monophasic or biphasic characteristics (Figure 3.6).

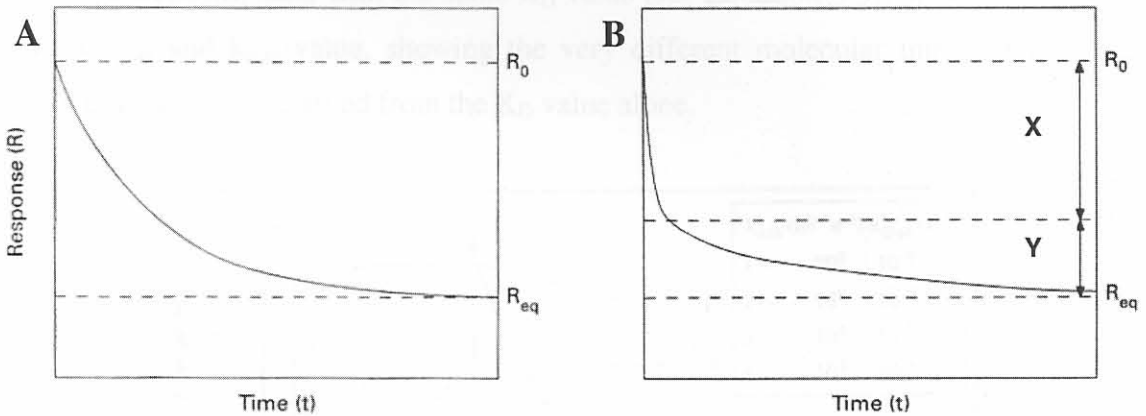


Figure 3.6: Theoretical dissociation curves (A) Monophasic. (B) Biphasic. R_0 is the initial response, R_{eq} the equilibrium response and X and Y in graph B denote the extents of the two phases. (Source: IASys, 1995b)

Similar to monophasic association, monophasic dissociation is described by the equation:

$$R_t = R_0 e^{-k_{diss}t} \quad (3.10)$$

where R_t is the amount of complex at time t , R_0 the initial complex concentration and k_{diss} the dissociation rate constant. Since k_{diss} is independent from ligate concentration, a single dissociation event can be used to determine k_{diss} . However, in practice, several different dissociation curves are compared to determine k_{diss} values.

Like association, dissociation curves may also be biphasic (see Figure 3.6) and is then described by:

$$R_t = Xe^{-k_{\text{diss}(1)}t} + Ye^{-k_{\text{diss}(2)}t} \quad (3.11)$$

where X and Y are the extents, and $k_{\text{diss}(1)}$ and $k_{\text{diss}(2)}$ the dissociation rate constants of the two individual and separate phases (see Figure 3.6). Once again, the second phase of dissociation most likely contain uninterpretable information; hence $k_{\text{diss}(1)}$ is used to determine a value for biphasic dissociations.

The big advantage of the IAsys biosensor method is that the rate constants are also determined as opposed to the equilibrium constants alone, as with other methods. This ability is very important as is illustrated in Figure 3.7. Four different theoretical interaction analyses are shown, each with the same K_D value (see Equation 3.5), but each also with a different k_{ass} and k_{diss} value, showing the very different molecular interactions of each system that cannot be derived from the K_D value alone.

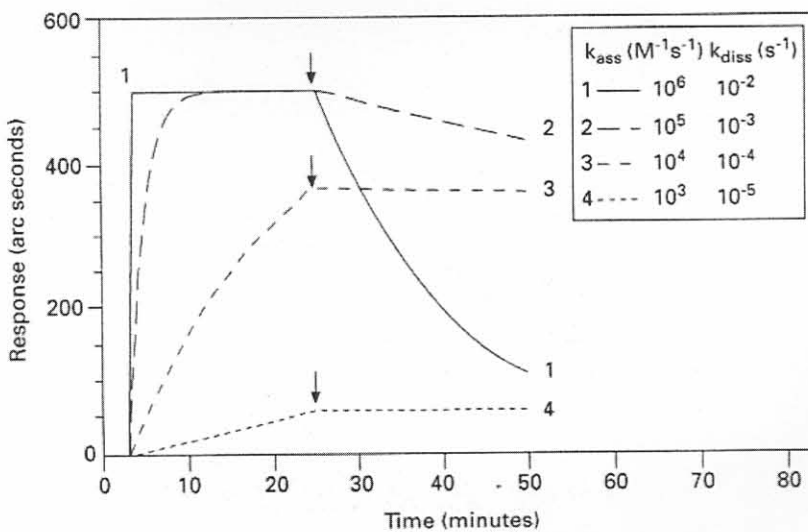


Figure 3.7: Association and dissociation curves of four theoretical molecular interactions. All four interactions have the same equilibrium constant ($K_D = 10^{-8}\text{M}$). The arrows indicate initiation of dissociation. (Source: IAsys, 1995b)

Therefore it can be assumed that the Interaction Analysis system (IASys) is ideal for the purpose of direct comparisons of affinity of CTxB for G_{M1} as a positive control. Due to the complex composition of patient sera, kinetic parameters cannot be derived for such samples, as they inherently contain contamination by other serum proteins and other molecules that may bind non-specifically.

3.2 Hypothesis

The optimised method for G_{M1} -liposome immobilisation on a biosensor can be applied to determine affinity characteristics of auto-antibodies involved in the Guillain-Barré syndrome.

3.3 Aims

- Determining statistically significant dissociation equilibrium constants (K_D) for cholera toxin B subunit binding to ganglioside G_{M1}
- Comparing acquired K_D values to published K_D values
- Optimising a method for relating patient serum reaction to G_{M1} -liposomes

3.4 Materials

The biosensor used was situated at the Department of Biochemistry, University of Pretoria, South Africa.

The liposomes were supplied by the biosensor manufacturer.

The patient sera were obtained from the Department of Neurology, University of Pretoria, South Africa.

The control sera were obtained from the Department of Biochemistry, University of Pretoria, South Africa.

The liposomes were supplied by the biosensor manufacturer.

The patient sera (five patients) were obtained from the Department of Neurology, University of Pretoria, South Africa. The control sera (five patients) were obtained from the Department of Biochemistry, University of Pretoria, South Africa. All sera were aliquoted and stored at -20°C until use. For interaction with liposomes were diluted between 50x and 100x with the running buffer (see pag 3.4.1) prior to injection into the cuvette chamber.

To overcome cross-reactivity between different serologic cells, the cells were calibrated by injecting 25 μl 1000x diluted control serum and allowing it to bind for five minutes at 37 $^{\circ}\text{C}$.

3.4 Materials and Methods

3.4.1 Materials

Monosialoganglioside G_{M1} from bovine brain, L- α -phosphatidylcholine, cholera toxin B subunit (CTxB) from *Vibrio cholerae* and bovine serum albumin (BSA) (Fraction V) from lecithin were from Sigma. Sodium chloride, anhydrous disodium hydrogen phosphate and potassium dihydrogen phosphate were from Merck. Analytical quality Tris and EDTA were from Saarchem and general purpose NaN_3 from BDH. Chemically pure KOH and analytical grade HCl were from Saarchem while analytical grade ethanol, chemically pure chloroform and general purpose NaOH were from BDH. Double-distilled deionised water was used for all analytical experiments. Saarchem, BDH and Merck products were supplied by Merck NT Laboratories, Darmstadt, Germany. Sigma products were supplied by Sigma-Aldrich Corp., St. Louis, Missouri, U.S.A.

3.4.2 Biosensors

The IAsys biosensor that was used was situated at the Department of Biochemistry, University of Pretoria, South Africa

Non-derivatised cuvettes were supplied by the biosensor manufacturer, IAsys Affinity Sensors, Cambridge, U.K.

3.4.3 Sera

Guillain-Barré syndrome patient sera (five patients) were a kind gift of Dr. Bart Jacobs, Department of Neurology, Erasmus University Rotterdam, Rotterdam, Netherlands. The sera were all ELISA positive for IgG antibodies and some of them were also IgM positive. All patients provided sera before commencement of treatment of the disease (F102A, F152A, F183A, F226A, F292A) and three of the patients provided sera six months after onset of the disease (F102E, F226F, F292E). Negative control serum was obtained from the investigator. All sera were aliquoted and stored at -70°C in cryovials. For interaction analyses, sera were diluted between 50 \times and 1000 \times with the running buffer (*see par 3.4.4*), prior to injection into the cuvette chamber.

To overcome discrepancies between different cuvette cells, the cells were 'calibrated' by injecting 25 μl 1000 \times diluted control serum and allowing it to bind for five minutes in both

cells. Only if the responses in both cells were the same, was the experiment continued, upon which another 25 μ l serum, either GBS or control, was injected at lower dilutions (100 \times) into the cells without aspirating.

3.4.4 Modification of running buffer

Cholera toxin B subunit was stored in a Tris-based buffer that could affect calculations due to its difference in refractive index in relation to PBS/AE. Accordingly, G_{M1}-liposomes and CTxB dilutions were carried out with a Tris-based buffer corresponding to the same concentrations as already contained in the CTxB. The Tris buffer contained 50mM Tris, 200mM NaCl, 3mM NaN₃, and 1mM Na₂EDTA (pH=7.5).

3.4.5 Ganglioside-liposome surfaces

Ganglioside-liposomes were prepared and immobilised as described (*see* Chapter 2, par 2.3.17 & 2.3.18). Throughout the experiments 5% G_{M1} (molar %) liposomes were used except where the effect of different concentrations of G_{M1} was tested on CTxB when 2, 5, 10, 14.3 and 20% were used. Regeneration was done as described (*see* Chapter 2, par 2.3.19).

3.4.6 Choleraenoid preparation and dilutions

Due to the biohazardous danger of working with a toxin, it was decided to use the non-toxic pentameric B subunit of CTx or choleraenoid (CTxB), the subunit responsible for binding to G_{M1}.

Five hundred micrograms of CTxB was dissolved in 500 μ l water, aliquoted into 50 μ l aliquots and stored at 4°C as prescribed by the suppliers. Upon use, an aliquot was diluted ten times with Tris buffer and then diluted again with Tris buffer to the desired concentrations. For statistical analysis, concentrations of 100-400nM with 50nM increments were prepared and used. This resulted in final CTxB concentrations of 50-200nM with 25nM increments.

3.4.7 Bovine serum albumin preparation and dilutions

It was assumed that BSA had an average molecular mass of 67 000Da. It was dissolved in Tris buffer and diluted to 20, 50, 100, 150 and 200nM with Tris buffer.

3.4.8 Interaction analysis

For the interaction analyses, baseline was maintained with 25 μ l Tris buffer for at least five minutes while a baseline event was entered in the event log. An association event was initiated upon the addition of 25 μ l of CTxB, BSA, control or patient serum dilutions. Association continued for five minutes, after which dissociation was initiated by washing five times with 60 μ l Tris buffer. Due to the high affinity of CTxB for G_{MI}-liposome surfaces, almost no dissociation occurred and derived dissociation rate constants were uninterpretable. Dissociation rate constants were therefore derived from the association data. Accordingly, no dissociations were done with CTxB and regeneration was done directly after associations.

3.4.9 FASTfit analysis

Kinetic parameters were determined using FASTfit software (IASys, 1996). Baseline, association and dissociation regions were selected so that all baseline, association and dissociation regions contained the same number of data points. At least 70% of association and dissociation curves were selected. Baselines were selected only during stable time frames. Every interaction analysis's parameters were calculated and fitted to theoretical mono- and biphasic kinetic curves and the best curve fit selected. Plots of $k_{on(1)}$ versus ligate concentration were obtained and used to derive the association and dissociation rate constants (k_{ass} and k_{diss}). The dissociation equilibrium constant, K_D , was accordingly calculated from these two rate constants.

3.4.10 Statistical analysis

To determine the best average kinetic parameters, three different sets of CTxB associations were done with the concentrations indicated (*see* par 3.4.6). The three sets were done on three different cuvettes. The experiment was duplicated in each cell and each cell represented a separate experiment. Consequently six different sets of data were used to determine the average $k_{on(1)}$ values. These were plotted against the final ligate (CTxB) concentration. Standard deviations of the average values were calculated and indicated. The slope and y-axis intercept were determined from a linear fit through the data points and these were used to derive the rate constants that were, in turn, used to determine a dissociation equilibrium constant.

3.5 Results

3.5.1 Suitability of cholera toxin as positive control

An important modification to the method when using CTxB was tested: CTxB is stored with a ready buffer mixture containing Tris, NaCl, NaN₃ and EDTA. Reconstituting the CTxB as prescribed by the manufacturers would result in a different buffer concentration as used for patient serum interaction analyses. As already mentioned (*see* Chapter 2 par 2.1.2.6), it is important that the buffer used for obtaining baselines in the biosensor be the same buffer used for preparing and diluting serum samples. The effect of the CTxB Tris-based buffer was tested and it was found that there are no significant effects on G_{M1}-liposome immobilisations, washings or regenerations (not shown).

In a preliminary experiment, four different concentrations of CTxB were used for interaction analysis on a surface created with liposomes containing 9PC:1G_{M1} (molar ratio) as described in Chapter 2 (*see* par 2.3.18), following the method as described in Annexure 2. The responses due to the different CTxB concentrations are shown in Figure 3.8.

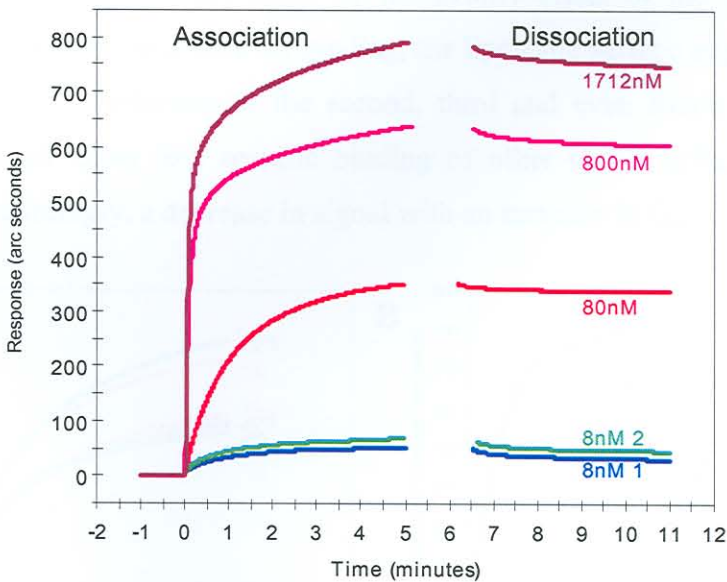


Figure 3.8: A FASTplot overlay showing the association and dissociation of different concentrations of CTxB (final concentrations) on an immobilised G_{M1}-liposome surface as obtained with an IAsys biosensor. The responses of the two interactions carried out with 8nM CTxB were almost identical and the other responses correlated with the CTxB concentration.

Two separate interaction analyses were done with the 8nM CTxB concentration (final concentration) to determine the reproducibility of the experiment. Both analyses gave the same low response as expected. Therefore, the use of CTxB as a positive control for GBS

patient serum antibodies against a G_{M1} -liposome biosensor surface was considered suitable.

3.5.2 Effect of ganglioside concentration in ganglioside-liposomes on cholera toxin B binding kinetics

To confirm the best concentration of G_{M1} to be used in G_{M1} -liposomes, a fixed concentration of CTxB (171nM) was injected over immobilised G_{M1} -liposome layers containing different amounts of G_{M1} ranging from 0-20% (molar percentage). As shown in Figure 3.8, it was observed that there was very little dissociation of CTxB from the surface and even some increase in signal, possibly due to re-association (not shown). Re-association of CTxB with G_{M1} on the surface is likely when loosely bound CTxB dissociates, thereby freeing G_{M1} molecules for association with other CTxB molecules with higher avidity. The result is a net increase in the signal during dissociation analyses.

Interestingly, a higher G_{M1} concentration did not correlate to the better binding of CTxB (Figure 3.9A). This could be explained by the avidity effect of the pentameric CTxB subunit. Having more G_{M1} available for binding, the liposome surface might bend a little to allow binding of G_{M1} molecules to the second, third and even fourth monomer of the subunit. This would allow less specific binding of other CTxB subunits due to steric hindrance and accordingly, a decrease in signal with an increase in G_{M1} concentration.

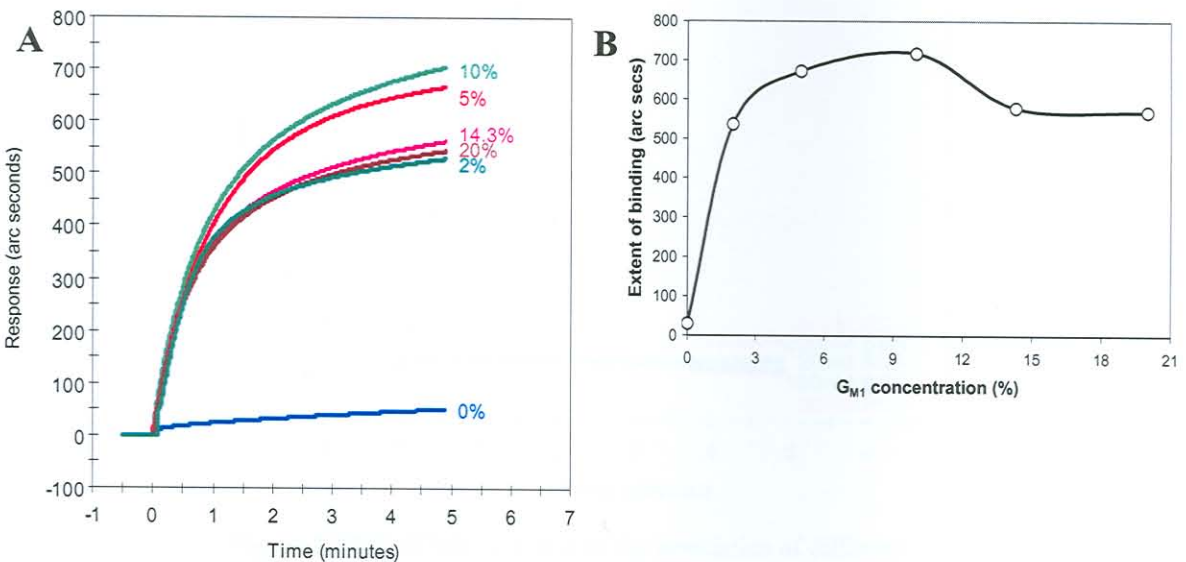


Figure 3.9: Association of 171nM CTxB to different G_{M1} concentrations on immobilised G_{M1} -liposomes. (A) FASTplot overlays. (B) Graph of G_{M1} percentage versus the total response. Percentages indicate the G_{M1} mole percentage in the immobilised liposomes.

At G_{M1} concentrations of 2%, the least binding of CTxB took place. The amount of CTxB that bound to the G_{M1} -liposome surface, appeared to be directly proportional to the G_{M1} concentration (Figure 3.9B), but reached a peak at about 10% before decreasing again to a lower plateau region. As expected, virtually no binding of CTxB to empty liposomes (pure PC) was observed. It was therefore concluded that molar concentrations higher than 5% G_{M1} in the liposomes had no significant advantage on CTxB binding, while G_{M1} concentrations at lower than 5%, evoked suboptimal binding of CTxB. Further experiments were continued with 5% G_{M1} -liposomes only.

3.5.3 Specificity of choleraenoid for ganglioside G_{M1}

It was necessary to test the possibility that non-specific association might create artefacts during interaction analyses of CTxB binding to G_{M1} -liposomes. Therefore, a 5% G_{M1} -liposome surface was immobilised and different concentrations of a non-specific protein (BSA) were injected as well as 100nM CTxB. As expected, very little BSA bound to the G_{M1} -liposome surface, even at twice the molar concentration of CTxB (Figure 3.10).

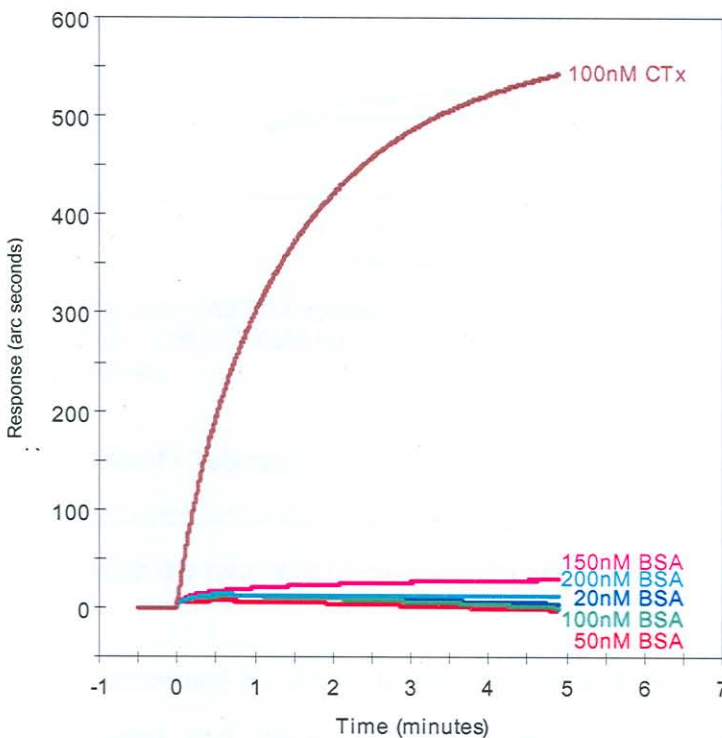


Figure 3.10: FASTplot overlays of the association of different BSA concentrations and 100nM CTxB to a G_{M1} -liposome surface measured with an IAsys biosensor.

Consequently, it was expected that non-specific interactions would have a negligible effect on the interaction analysis profiles.

To confirm the specificity of CTxB for G_{M1} , identical concentrations (200nM) of both CTxB and BSA were prepared and injected separately over a 5% G_{M1} -liposome or PC-liposome surface (Figure 3.11). Results indicated that the only high response was when CTxB was injected over the G_{M1} -liposome surface. When CTxB was injected over a PC-liposome surface, a negligible amount bound and BSA associated only negligibly to either surfaces, indicating that the specific binding of CTxB to G_{M1} can be measured quantitatively on the IAsys biosensor using immobilised G_{M1} -liposomes.

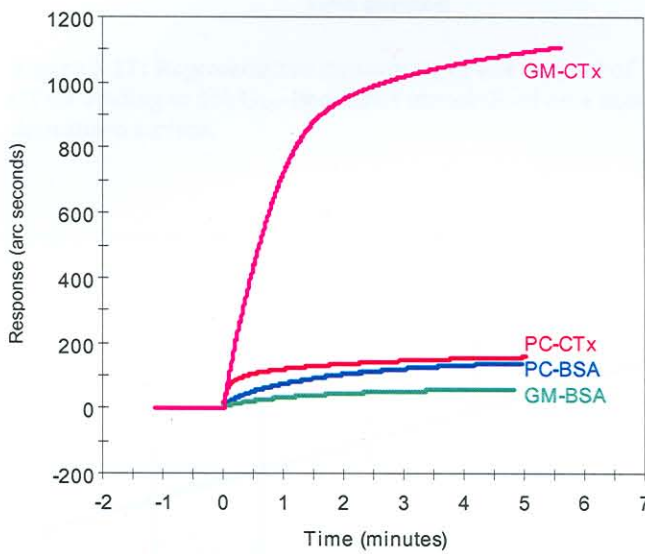


Figure 3.11: FASTplot overlays of the associations of 200nM CTxB or 200nM BSA with 5% G_{M1} - or pure PC-liposomes.

3.5.4 Statistical analysis of choleraenoid binding kinetics

Six sets of binding kinetics similar to that illustrated in Figure 3.12, were generated using three different cuvettes, with the two cells of each cuvette representing a separate data set.

The $k_{on(1)}$ values were determined by FASTfit analysis for each data set separately. The values were then averaged and plotted onto a graph of $k_{on(1)}$ versus the ligate concentrations (Figure 3.13).

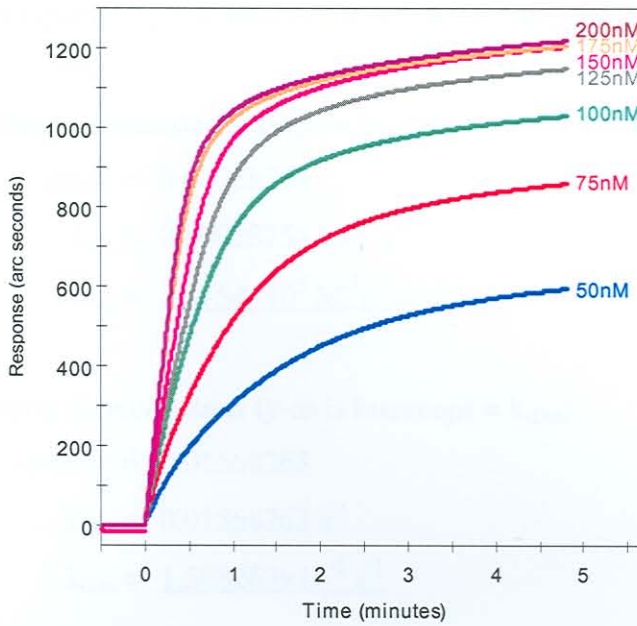


Figure 3.12: Representative sensorgram of one data set of CTxB binding to 5% G_{M1} -liposomes immobilised on a non-derivatised surface.

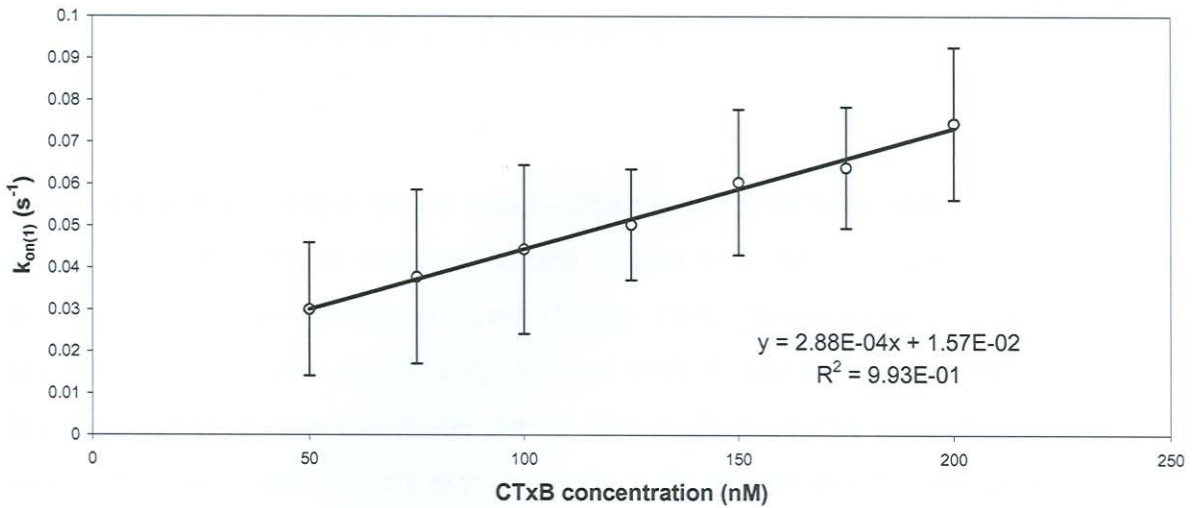


Figure 3.13: Plot of the first order apparent on-rate ($k_{on(1)}$) versus ligate concentration for the binding of CTxB to a 5% G_{M1} -liposome surface. The linear fit through the data points is illustrated and the slope, intercept and quality of the fit, expressed as an R^2 value, is shown.

The slope and y-axis intercept of the linear fit were used to calculate the association and dissociation rate constants respectively (*see* Equation 3.7):

Linear fit equation: $y = 0.00028754x + 0.01568263$

Association rate constant (slope = k_{ass})

$$\text{slope} = 0.00028754$$

$$\therefore k_{\text{ass}} = 0.00028754 \text{ nM}^{-1}\text{s}^{-1}$$

$$\therefore k_{\text{ass}} = \underline{2.8754 \times 10^5 \text{ M}^{-1}\text{s}^{-1}}$$

Dissociation rate constant (y-axis intercept = k_{diss})

$$\text{y-axis intercept} = 0.01568263$$

$$\therefore k_{\text{diss}} = 0.01568263 \text{ s}^{-1}$$

$$\therefore k_{\text{diss}} = \underline{1.568263 \times 10^{-2} \text{ s}^{-1}}$$

Using Equation 3.5, these rate constants can be used to determine the K_D value:

$$\begin{aligned} K_D &= k_{\text{diss}} / k_{\text{ass}} \\ &= 1.568263 \times 10^{-2} \text{ s}^{-1} / 2.8754 \times 10^5 \text{ M}^{-1}\text{s}^{-1} \\ &= \underline{5.45 \times 10^{-8} \text{ M}} \end{aligned}$$

3.5.5 Exploratory experiments with Guillain-Barré syndrome patient sera

Initial serial experiments with patient and control sera indicated that the capacities of binding are not significantly different (Figure 3.14). However, the slopes of the two association events were significantly different with the patient's initial association curve being much steeper than that of the control. This might be due to the higher percentage of specific G_{M1} antibodies that are expected to be in the patient sera. Serial experiments were carried out in preference to parallel experiments with the patient and control sera in either of the two cuvette cells, due to earlier observations that the two cells of one cuvette sometimes do not provide the same response to the same solutions (*see* Chapter 2, Table 2.1) and cannot be compared directly.

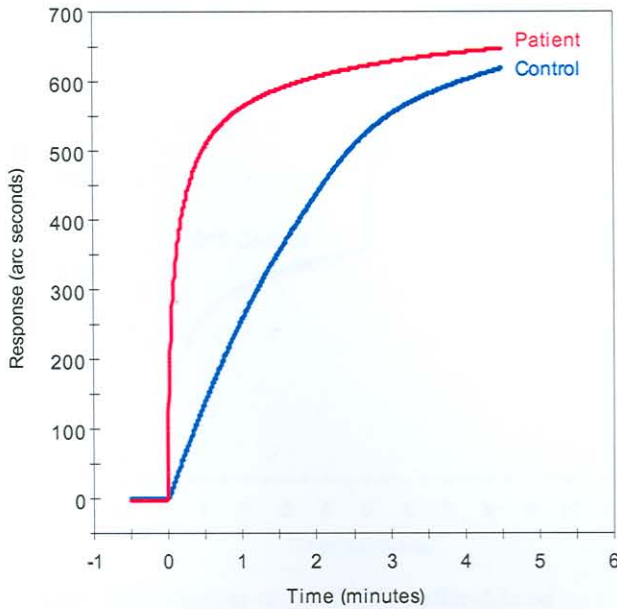


Figure 3.14: Binding of 1:50 Tris-buffer-diluted control and patient (F102A) sera to a 5% G_{M1} -liposome surface. The sensorgram is representative of two serial experiments in the same cell.

An improvement on this method was suggested where control serum is used at a very low concentration to calibrate the two cells. Typically, a sample volume of 1000 \times diluted control serum is added to both cells after liposome immobilisation and only if the response to this addition is identical in the two cells, a further addition is made with less diluted patient and control sera in the respective control and test cells.

In Figure 3.15 it is shown that initial non-specific binding of control serum was identical in both cells but the difference between the subsequent patient and control sera added on top of the ‘calibration binding’ was significantly different. The control and test cells were also alternated to determine if the higher binding of the patient serum was not artefactual. Even in alternated cells the patient sera showed significantly higher binding compared to the control serum (not shown). Due to the heterogeneity of sera and the required calibration step on the biosensor, it may prove difficult to quantify specific antibody binding directly from serum using the biosensor. However, the biosensor technique might be employed to semi-quantitatively distinguish among patients using the calibration bindings to determine a ratio of binding that may be compared among patient and control sera.

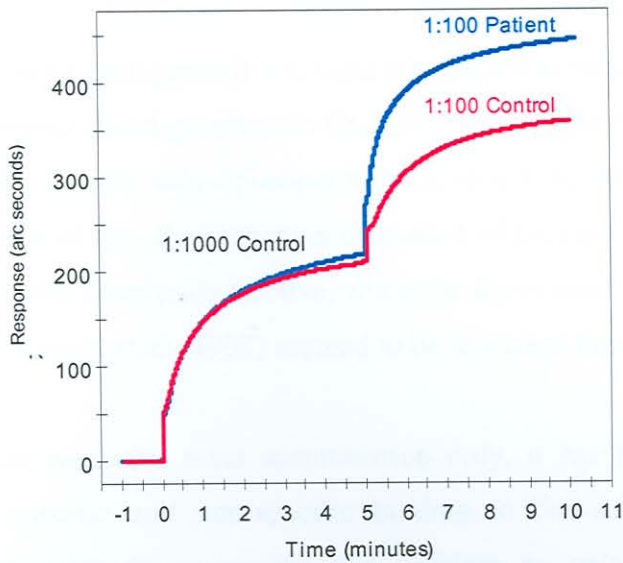


Figure 3.15: Binding of 1:100 Tris-buffer-diluted control and patient sera (F102A) after calibration with 1:1000 Tris-buffer-diluted control serum to a 5% G_{M1} -liposome surface.

It was not yet possible to calculate absolute K_D values for the binding of patient and control sera to immobilised G_{M1} -liposome surfaces, as was done with the CTxB (positive control) binding to the same surfaces. This is primarily due to the fact that the absolute antibody concentrations in the sera were unknown and variable among patients. Furthermore, there are antibodies against other types of gangliosides like G_{A1} and G_{D1a} that would result in complex cross-reactivity patterns. There is also the different avidities to consider between the different antibody isotypes present in all human sera.

For further characterisation it would be necessary to isolate specific isotypes with singular specificities as Ab1, before they can be immobilised and Ab2 antibodies against the Ab1 antibodies characterised. It would also be necessary to increase the number of control sera to produce a statistically significant background against which the different antibody sets could be measured.

3.6 Discussion

Cholera toxin B subunit (cholera toxin B subunit) was used to standardise conditions for the specific binding of ligate to immobilised ganglioside G_{M1} . Preliminary experiments indicated that CTxB bound optimally to a 5% G_{M1} -liposome surface, similar to other studies (Kuziemko *et al.*, 1996). In the light of this, the higher concentration of G_{M1} used by Athanassopoulou *et al.* (1999) was probably counter-productive, while the lower concentrations of G_{M1} used by other studies (MacKenzie *et al.*, 1997) seemed to be less ideal than 5%.

Because the biosensor measures mass accumulation only, it has no way of telling the difference between specific and non-specific binding to the surface. Enzyme-linked immunosorbent assay methods circumvent this problem by using a specific reporter antibody that recognises bound antibody specifically. A disadvantage of ELISA is that it is unable to measure low affinity antibodies. In addition, it cannot determine rate constants as it measures only end-point equilibrium data, compared to real-time measurements with the biosensor. Results presented here conclusively show that CTxB binds specifically to G_{M1} and that it is not necessary to confirm this with ELISA techniques, as may have been desirable with antibody binding.

The K_D value for binding of CTxB to G_{M1} under the optimised conditions was determined to be $5.45 \times 10^{-8} M$. Other laboratories have also determined K_D values for the binding of CTxB to G_{M1} using various biosensors or isothermal titration calorimetry (ITC). Their results are summarised in Table 3.3:

Table 3.3: Comparison of K_D values obtained by different laboratories

Method	G_{M1} molar %	k_{ass} ($M^{-1}s^{-1}$)	K_D (M)	Reference
IASys biosensor, lipid monolayer on hydrophobic cuvettes	25	N.A.	3.00×10^{-8}	(Athanassopoulou <i>et al.</i> , 1999)
BIACore biosensor, lipid bilayers on non-derivatised chips	5	1.27×10^6	4.61×10^{-12}	(Kuziemko <i>et al.</i> , 1996)
BIACore biosensor, LPS containing lipid bilayer captured by IgG immobilised on CMD chip	2	6.2×10^5	7.3×10^{-10}	(MacKenzie <i>et al.</i> , 1997)
Isothermal titration calorimetry	2	N.A.	1.37×10^{-8}	(Masserini <i>et al.</i> , 1992)
IASys biosensor, lipid bilayers on non-derivatised cuvettes	5	2.88×10^5	5.45×10^{-8}	This study

N.A. – Not available

The K_D value determined in this study, correlates very well with the two published values that were also determined using an IAsys biosensor. Two of the values in Table 3.3 do not correlate well with IAsys results. In the first instance by Kuziemko *et al.*, (1996), who determined a K_D of $4.61 \times 10^{-12} \text{M}$ using the BIAcore biosensor, the authors used $k_{\text{diss}(2)}$ instead of $k_{\text{diss}(1)}$ to determine the K_D which they claim to be a result of non-specific interactions. However, they have determined $k_{\text{diss}(1)}$ as well, and when this value is used instead of the $k_{\text{diss}(2)}$, a K_D value of $7.03 \times 10^{-9} \text{M}$ is obtained, much closer to the published values of Athanassopoulou *et al.* (1999) and Masserini *et al.* (1992). In the second instance (MacKenzie *et al.*, 1997) the authors used a 2% molar concentration of G_{M1} in their lipid bilayer on the BIAcore instrument as well as smaller concentrations of CTxB. At these lower concentrations the pentavalent binding capability of CTxB is probably better determined. As a consequence, CTxB will dissociate slower, leading to a higher k_{diss} value and, in turn, a lower calculated K_D value.

The ITC of Masserini *et al.* (1992) is probably the best technique to determine kinetic parameters because it measures these parameters in free solution while ligand-ligand pairs are in their native states. This is opposed to the biosensor technique that measures binding to immobilised ligand under very different concentration ranges. This is in contrast to ITC where the molecules are in similar concentration ranges and parameters determined from interactions in free solutions (Masserini *et al.*, 1992; Jelesarov & Bosshard, 1999; Menze *et al.*, 2001). Therefore it can be considered to be the standard against which to measure values obtained by other methods. A possible disadvantage is that affinity constants are calculated from the measured heat that is released during a molecular recognition reaction. Unless the recognition mechanism between the ligand-ligand pair is very simple and defined, the total measured heat is a global heat – that includes the energy of chemical transformation following the recognition interactions, should this be a result of the interaction. The K_D determined in this study, where no chemical transformation during recognition is anticipated, does not compare badly to the ITC results of Masserini *et al.* (1992).

The K_D value obtained by Athanassopoulou *et al.* (1999), also using the IAsys biosensor, is in very good agreement with the value obtained here. The authors used a much higher G_{M1} concentration and also used a different method of immobilising the G_{M1} molecules. Exploratory experiments using the same method employed by these authors were

problematic as it was impossible to maintain stable baselines when working with hydrophobic cuvettes (not shown). The method of immobilising G_{M1} -liposomes on a non-derivatised surface used in the current study is not only more reliable, but also mirrors the normal molecular and physiological environments of G_{M1} better than when G_{M1} is immobilised on a hydrophobic cuvette. During such an immobilisation, G_{M1} is subjected to relatively harsh conditions with iso-propanol.

The method employed by Mackenzie *et al.* (1997) on the BIAcore biosensor may provide a more interesting perspective on CTxB binding kinetics and subsequent affinity and avidity measurements, as a much slower dissociation rate is observed with the lower concentrations of both CTxB and G_{M1} employed by them. Inspection of the association rate constants of two of these studies (Kuziemko *et al.* (1996): $1.27 \times 10^6 \text{ M}^{-1}\text{s}^{-1}$ and Mackenzie *et al.* (1997): $6.2 \times 10^5 \text{ M}^{-1}\text{s}^{-1}$) indicate that the association rate constant, k_{ass} , calculated by our method ($2.88 \times 10^5 \text{ M}^{-1}\text{s}^{-1}$) is within one logarithmic unit of the published BIAcore values (Table 3.3). The other two studies (Masserini *et al.*, 1992; Athanassopoulou *et al.*, 1999) did not indicate their k_{ass} values for comparison. In the Introduction of this Chapter the desirability to consider not only the equilibrium constant on its own, but also the rate constants was emphasised, as is evident from the results obtained here when comparing patient and healthy control sera. It was determined that both sera bound with the same capacity, but not the same vigour.

Standard deviations for the apparent on-rate versus ligate concentration plot determined here, are relatively large despite the linear regression fit being very accurate. The main reason for this might be that three different cuvettes were used to get a value closer to the average.

In conclusion, the method for measuring and comparing the anti- G_{M1} -antibody binding kinetics of GBS patient sera at different stages of the disease and especially after recovery, using the method described here, seems to be entirely feasible. This should corroborate the studies by Lundkvist *et al.* (1993) and provide better insight for studying the idiotype network's role in GBS.